Ultrathin $SrTiO_3$ films: epitaxy and optical properties

2009 J. Phys.: Condens. Matter 21 232203

(http://iopscience.iop.org/0953-8984/21/23/232203)

IOP FTC
IOP PUBLISHING JOURNAL OF PHYSICS: CONDENSED MATTER
J. Phys.: Condens. Matter **21** (2009) 232203 (6pp) doi:10.1088/0953-8984/21/23/232203

FAST TRACK COMMUNICATION

Ultrathin $SrTiO_3$ films: epitaxy and optical properties

M Tyunina[1,4], J Narkilahti[1], J Levoska[1], D Chvostova[2], A Dejneka[2], V Trepakov[2,3] and V Zelezny[2]

[1] Microelectronics and Materials Physics Laboratories, University of Oulu, PL4500, FI-90014 Oulun yliopisto, Finland
[2] Institute of Physics, Academy of Sciences of the Czech Republic, Na Slovance 2, 182 21 Prague 8, Czech Republic
[3] Ioffe Physical-Technical Institute of the RAS, 194 021 St Petersburg, Russia

E-mail: marinat@ee.oulu.fi

Received 21 April 2009
Published 11 May 2009
Online at stacks.iop.org/JPhysCM/21/232203

Abstract

Ultrathin (12–15 nm) $SrTiO_3$ films are grown by pulsed laser deposition on various single-crystal substrates. The crystal structure, orientation, and strain state of the films are studied by x-ray diffraction. The room-temperature optical properties of the films are experimentally determined using ellipsometric spectroscopy in the 1–6 eV spectral range. Epitaxial films with biaxial in-plane strain are obtained on $LaAlO_3$, $DyScO_3$, and $KTaO_3$ substrates, with the critical thickness for pseudomorphic growth being less than 10 nm. Abrupt strain relaxation has been detected.

The optical properties of the films with different microstructure are compared with each other and with those of single-crystal $SrTiO_3$. Based on the comparison, surface effects are suggested to be dominant in the visible range, while the interband transitions are smeared and suppressed due to small film thickness and the presence of biaxial strain. The energies of gaps can increase due to strain-induced polarization. The absorption edge is affected by all the factors mentioned (surface, thickness, strain, and polarization).

1. Introduction

Strontium titanate ($SrTiO_3$, STO) is an ABO_3-type perovskite and can exhibit ferroelectric (FE) behavior. STO is a quantum paraelectric, in which FE behavior can be induced by appropriate doping, through oxygen isotope exchange, or under applied stress. Recently, special attention has been paid to STO thin films, which appeared to be attractive for integrated microelectronic and optoelectronic devices due to growth that is compatible with Si technology [1]. The low- and high-frequency dielectric properties of thin-film STO have been extensively studied. In contrast to this, studies of the optical properties and band structure are rather limited. Compared to single-crystal STO, studies of thin films [2] have revealed a decrease in the index of refraction in the visible range, a shift of the absorption edge to higher energies, and smearing of interband transitions. This has been ascribed to microstructural features such as grain boundaries, amorphous layers, and possible nonstoichiometry. These features are absent in high-quality single-crystal epitaxial films.

In heteroepitaxial films, due to the mismatch of the in-plane (parallel to the substrate surface) lattice parameters a_F of the film material and a_S of the substrate, a misfit strain s can arise: $s = (a_S - a_F)/a_F$. With increasing film thickness d, the strain s relaxes mainly through the formation of misfit dislocations. Moreover, the strain can relax through development of morphological instabilities (surface roughening). In perovskite FEs, it can also relax through possible formation of FE domains. Although mechanisms of strain relaxation in perovskite FE films are still under discussion, it has been demonstrated that misfit strain can be completely sustained in STO films without relaxation if

[4] Author to whom any correspondence should be addressed.

Table 1. Substrate material, its lattice parameter a_s, and calculated in-plane misfit strain s in STO films assuming pseudomorphic growth.

Substrate	a_s (Å)	s (%)
MgO(001)	4.216	8
$LaAlO_3$(001)	3.789	−3.0
$DyScO_3$(011)	3.944	1
$KTaO_3$(001)	3.989	2.2

the film thickness is smaller than a certain critical thickness d_{CRIT}, in the range of several nanometers [3]. For $d > d_{CRIT}$, a gradual strain relaxation has been suggested [4]. In ultrathin STO films with large enough biaxial in-plane strain, onset of the FE state has been theoretically predicted [5] and experimentally detected [3, 6–9].

Compared to calculations of the band structure of STO performed long ago [10], recent progress in first-principles analysis has brought a better understanding of the electronic structure of single-crystal STO and the STO surface [11]. However, the effects of strain, possible polarization, surface, and thickness on the band structure and optical properties of the films have not yet been analyzed. The present experimental work deals with these poorly studied effects. STO films with a thickness below 15 nm were grown on different substrates. Their room-temperature crystal structure and optical properties were experimentally determined and analyzed. To our knowledge, studies of the optical properties of ultrathin strained epitaxial STO films have not been reported so far.

2. Experiment

For STO films, single crystals of Al_2O_3(0001), MgO(001), $LaAlO_3$(001), $DyScO_3$(011), and $KTaO_3$(001) were used as substrates. The lattice parameters a_S of the substrates assuming a pseudocubic structure of the substrate surface and the estimated expected misfit strain s in STO films are listed in table 1. For strain estimation, the cubic crystal structure of STO with the lattice parameter 3.905 Å is considered. For a sapphire substrate (not listed in table 1), a good match of the STO(111) planes with the Al_2O_3(0001) oxygen planes exists, suggesting the possibility of growth of strain-free (111) oriented STO films.

The STO films were grown by *in situ* pulsed laser deposition (PLD) in oxygen ambient at a temperature of 943 K. The crystal structure of the films was studied by x-ray diffraction using Cu Kα radiation with a post-monochromator. The crystal orientation, epitaxy, strains, and crystal perfection were analyzed using Θ–2Θ and ω–2Θ scans, and ω rocking curves. To confirm in-plane epitaxy and determine the lattice parameters of STO films, the (004) perovskite reflection in Θ–2Θ scans and reciprocal space maps in (004), (024), and (033) STO directions were inspected. For the maps, the contribution of Cu Kα_2 radiation to the total intensity was eliminated by Rachinger correction. Using substrates as reference, the out-of-plane and in-plane lattice parameters of STO films, c_{STO} and a_{STO}, were found with an accuracy of ±0.0005 Å and ±0.001 Å, respectively.

To study the in-plane optical properties of STO films, ellipsometric spectra were collected using a variable-angle spectroscopic ellipsometer (J A Woollam) operating in the range of photon energies $E = 1$–6 eV (wavelength $\lambda \sim 1200$–200 nm). The main ellipsometric angles ψ and Δ were measured in the reflection mode at three angles of incidence (65°, 70°, and 75°). To eliminate depolarizing effects of the back-surface reflection from the substrate, the back surface was mechanically roughened. The spectra were analyzed with the WVASE32 software package considering a stack of semi-infinite substrate, STO film, surface roughness, and ambient air, and using the generalized multi-oscillator model. To increase the accuracy of the analysis, the bare substrates were also studied separately.

3. Results and discussion

3.1. Crystal structure

The epitaxial perovskite STO films with (001) planes parallel to the substrate surfaces were obtained on $LaAlO_3$, $KTaO_3$, and $DyScO_3$ (figures 1(a)–(c)). The epitaxial relationship is STO[100](001) ∥ $KTaO_3$[100](001), STO[100](001) ∥ $LaAlO_3$[100](001), and STO[100](001) ∥ $DyScO_3$[110](011).

In STO/MgO (figure 1(d)), the misfit is very large, and can induce the Volmer–Weber (island) growth mode instead of the Frank–van der Merwe (layer-by-layer) mode. Indeed, as evidenced by atomic force microscopy (AFM) inspection, the growth of relaxed perovskite STO(001) films with $c_{STO} \approx 3.910$ Å is accompanied by considerable surface roughening. Correspondingly, the full width at half maximum (FWHM) of the (002) rocking curve is large: FWHM(002) ≈ 3.15°. It is known that development of morphological instabilities can be reduced by adjusting the surface energies of the substrate and the growing film. This can be achieved, for instance, by controlling the deposition rate [12] and/or the substrate temperature. In PLD, control of the growth rate can be realized by varying the density of laser radiation, the ambient pressure, the target-to-substrate distance, and the pulse repetition rate. However, in STO/MgO, a large lattice misfit is dominant and it prohibits epitaxial layer-by-layer growth of STO at all surface energies.

The importance of a good match between surface energies of the substrate and growing film is evidenced in the growth of STO on Al_2O_3. Despite the good match of the STO(111) planes with the Al_2O_3(0001) oxygen planes, a randomly oriented polycrystalline STO film is grown on Al_2O_3(0001) (figure 1(e)). The Volmer–Weber growth of polycrystalline STO can be explained by a possibly smaller surface energy of Al_2O_3 compared to that of STO.

For epitaxial STO films on $LaAlO_3$, $DyScO_3$, and $KTaO_3$ substrates, the Θ–2Θ patterns in the vicinity of (002) peaks of STO are shown in more detail in figure 2. The satellites around (002) reflections are the peaks of the Laue function due to the small thickness of high-quality smooth crystalline films.

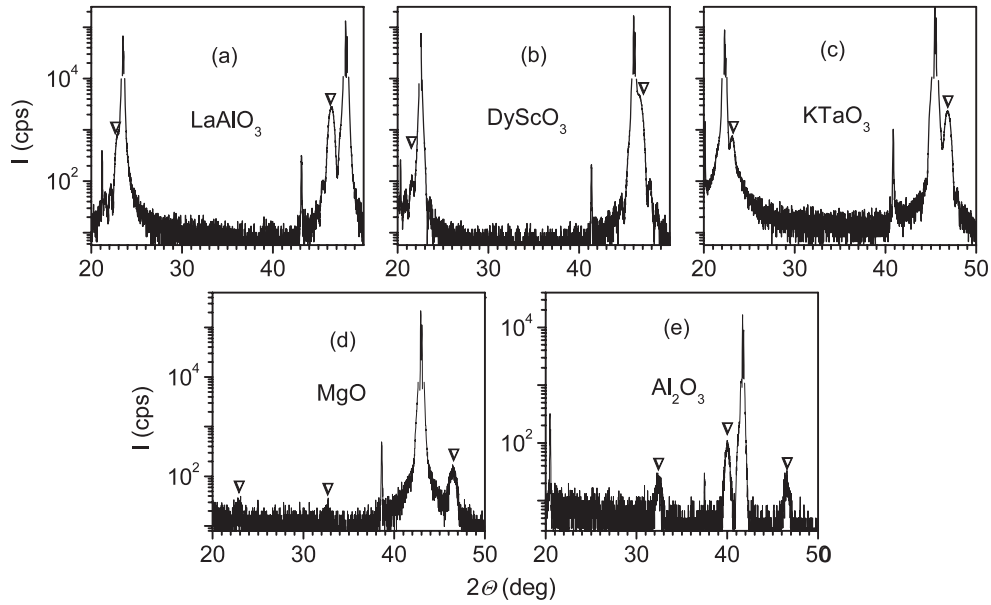

Figure 1. Θ–2Θ x-ray diffraction patterns of STO films grown on (a) $LaAlO_3$, (b) $DyScO_3$, (c) $KTaO_3$, (d) MgO, and (e) Al_2O_3 substrates. The intensity of substrate reflections (except K_β) is reduced by filtering. STO reflections are marked by triangles.

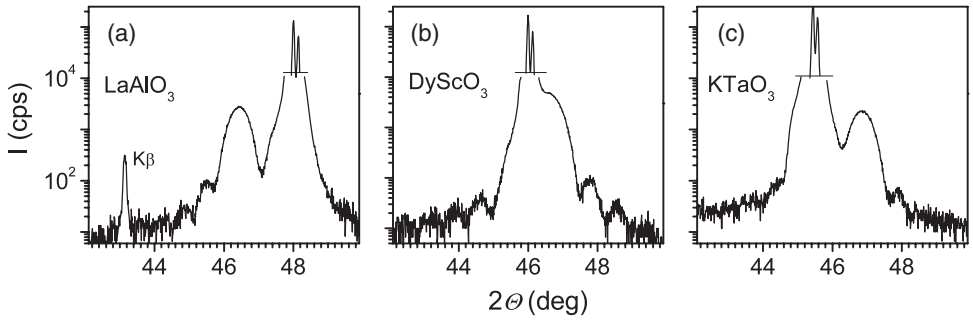

Figure 2. Θ–2Θ x-ray diffraction patterns of STO films on (a) $LaAlO_3$, (b) $DyScO_3$, (c) $KTaO_3$, substrates are shown in the vicinity of STO(002) reflections. The intensity of substrate reflections (except K_β) is reduced by filtering (as shown by straight lines).

The thickness d of STO films is determined from the positions of minima of the Laue function using numerical simulations of kinematic diffraction intensity. The thickness is equal to $d = 147$, 123, and 130 Å for STO films on $LaAlO_3$, $DyScO_3$, and $KTaO_3$ substrates, respectively.

The out-of-plane and in-plane lattice parameters of STO/$LaAlO_3$ are found to be $c_{STO} \approx 3.913$ Å and $a_{STO} \approx 3.895$ Å. The in-plane biaxial strain s_{STO} in the deposited STO films is defined as $s_{STO} = (a_{STO} - a_0)/a_0$, where a_0 is the lattice parameter of bulk STO. In STO/$LaAlO_3$ the in-plane compressive strain is $s_{STO} = -0.25\%$, considerably smaller than the expected one. However, it is in line with that of -0.54% previously obtained in 10 nm thick STO [3]. The critical thickness is $d_{CRIT} < 10$ nm, with a profound strain relaxation in the 15 nm thick film. The rocking curve FWHM(004) $\approx 0.09°$ is consistent with this. It is known that at 708 K, single-crystal $LaAlO_3$ experiences a cubic-to-rhombohedral structural phase transition with the formation of twins. For $LaAlO_3$ substrates, the structural phase transition, the presence of low-angle twin boundaries, and the related morphology of the substrate surface create an additional route for strain relaxation in the grown STO film during cooling.

In epitaxial STO films on $KTaO_3$ and $DyScO_3$, the (004), (024), and (033) rocking curves are found to be as narrow as those of the substrates, being determined mainly by the instrumental broadening. In STO/$DyScO_3$, the lattice parameters are $a_{STO} \approx 3.938$ Å and $c_{STO} \approx 3.885$ Å with the in-plane strain being, respectively, $s_{STO} \approx 0.85\%$. This agrees with the previously obtained strain of 0.8% in 50 nm thick STO/$DyScO_3$ [6]. In STO/$KTaO_3$, the lattice parameters are found to be $c_{STO} \approx 3.864$ Å and $a_{STO} \approx 3.987$ Å. The in-plane parameter a_{STO} is close to that of the substrate $a_S = 3.989$ Å. The obtained tensile strain $s_{STO} \approx 2.1\%$ is consistent with the expected $s = 2.2\%$ and that previously obtained in 7 nm thick film [3].

In STO/$KTaO_3$, however, a more careful inspection of the (033) point in the reciprocal lattice (figure 3) reveals the presence of another maximum with $a_{STO} \approx 3.972$ Å, $c_{STO} \approx 3.876$ Å, and $s_{STO} \approx 1.7\%$. Such a magnitude of tensile strain s_{STO} corresponds to that reported for a 20 nm thick film [3].

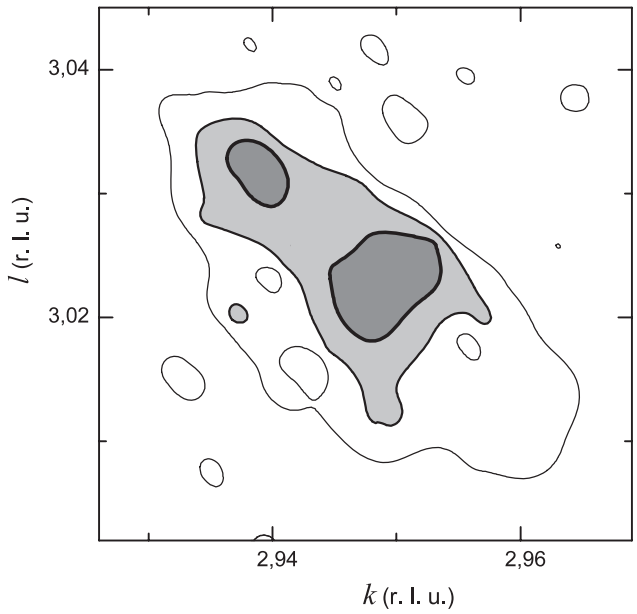

Figure 3. Reciprocal space map of STO/$KTaO_3$ around (033) reflections on the (0kl) $KTaO_3$ reciprocal lattice plane.

The studied 13 nm thick STO/$KTaO_3$ film contains both a strongly strained near-interface fraction and a partly relaxed near-surface fraction. The presence of two distinct (033) maxima implies rather abrupt strain relaxation. Considering the results of [3] and the present work, the critical thickness d_{CRIT} of STO on $KTaO_3$ can be in the range 7 nm $< d_{CRIT} <$ 13 nm.

The results of x-ray diffraction analysis evidence that for epitaxial growth of strained STO, a delicate match between substrates and STO films, including their lattices and surface energies, is required. Besides that, in the film grown at a high deposition temperature, strain relaxation during cooling is shown to be important too. Remarkably, the possibility of abrupt strain relaxation is detected. The critical thickness d_{CRIT}, below which epitaxial STO films grow pseudomorphically with the substrate surface, is found to be $d_{CRIT} < 10$ nm for $LaAlO_3$(001) substrates, $d_{CRIT} < 12$ nm for $DyScO_3$(011) substrates, and 7 nm $< d_{CRIT} < 13$ nm for $KTaO_3$(001) substrates.

3.2. Optical properties

In the grown STO films, the room-temperature optical index of refraction n and the extinction coefficient k are obtained as a function of photon energy E (figure 4) using ellipsometric spectra. The correctness of the applied spectral analysis is confirmed by the good agreement between STO thickness extracted from ellipsometric data and that extracted from x-ray diffraction intensity. The room-temperature optical properties of STO films with different microstructure and strain state are compared with each other and with the properties of the single-crystal STO [13]. This makes it possible to reveal the effects of surface, thickness, and strain on the optical behavior in STO films.

As seen from figure 4, the magnitude of n is noticeably affected by the STO surface. In the visible part of the spectra, the largest difference between n in films and crystal is observed in STO/MgO and STO/$LaAlO_3$. In STO/MgO this agrees with the development of morphological instabilities detected by AFM. Although such surface roughening is absent in STO/$LaAlO_3$, the presence of low-angle twin boundaries in $LaAlO_3$ and the related morphology of $LaAlO_3$ and STO surfaces can affect the measured n. In contrast, in the smooth epitaxial STO/$DyScO_3$ and STO/$KTaO_3$ compared to single-crystal STO, a decrease of n in the visible range is less pronounced and it cannot be unambiguously ascribed to surface effects. Rather, it might be connected with changes in band structure of the film body, since the whole n spectrum changes (figures 4(c) and (d)).

The influence of thickness can also be seen in figure 4. In all STO films, in the ultraviolet range $E > 3.8$ eV, the spectra of both n and k are smeared compared to those in the crystal. The smearing is independent of surface roughening or strain. Such a smearing might be interpreted as resulting from a broadening of critical points of Brillouin zone due to scattering of the electron Bloch waves [14]. Correspondingly, direct optical transitions associated with X, Γ, and M points of Brillouin zone can become smeared.

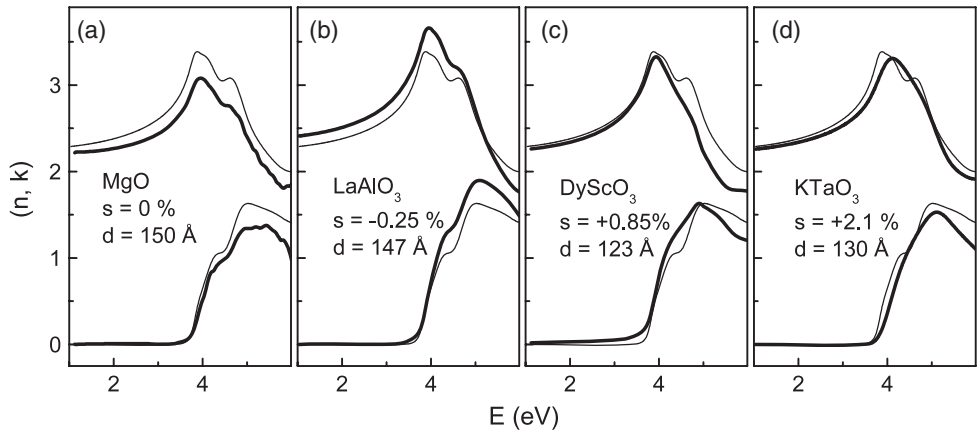

Figure 4. Index of refraction n (topmost lines) and extinction coefficient k (lower lines) as a function of photon energy E in STO films on (a) MgO, (b) $LaAlO_3$, (c) $DyScO_3$, and (d) $KTaO_3$ substrates. For comparison, the properties of single-crystal STO are also shown by thin lines.

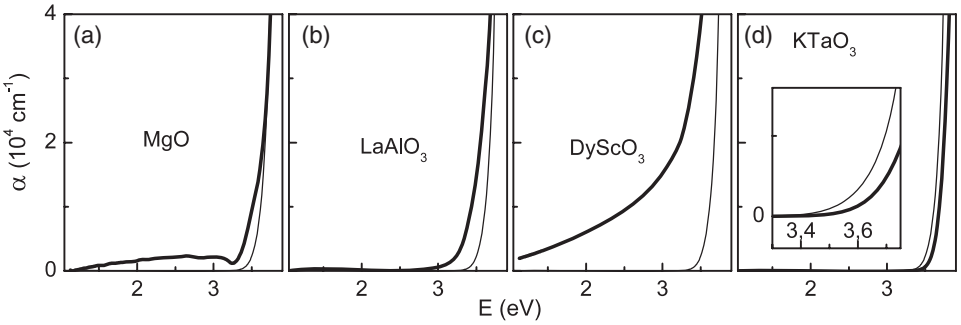

Figure 5. Absorption coefficient α as a function of photon energy E in STO films on (a) MgO, (b) $LaAlO_3$, (c) $DyScO_3$, and (d) $KTaO_3$ substrates. For comparison, properties of single-crystal STO are also shown by thin lines. The inset in (d) shows the near-edge absorption in STO/$KTaO_3$.

In addition to the spectral smearing, in the strained STO/$DyScO_3$ and STO/$KTaO_3$ a relative suppression of the interband X–X transitions is evidenced by the evolution of both n and k spectra at $E > 4.2$ eV (figures 4(c) and (d)). With increasing tensile in-plane strain s, the suppression becomes more profound. For large enough tensile strain, a noticeable increase in the energies of transitions can also be seen. Indeed, compared to STO crystal and STO/$DyScO_3$, in the strongly strained STO/$KTaO_3$ the (n, k) spectra are shifted to higher photon energies. It should be noted that in perovskite FEs, the FE transition and the appearance of spontaneous polarization with long-range order has been shown to result in an increase in the energies of optical gaps [14]. In STO/$KTaO_3$, the possible high-temperature strain-induced FE transition might explain the observed shift of the (n, k) spectra. Also in STO/$DyScO_3$, a strain-induced FE transition is possible [6]. However, due to smaller s it can take place at lower temperatures than in STO/$KTaO_3$ (for instance, below room temperature) and cannot affect the room-temperature optical properties.

The absorption coefficient $\alpha = 4\pi k/\lambda$ is presented as a function of photon energy $E < 4$ eV in figure 5. In STO/MgO and STO/$LaAlO_3$, the surface effect on absorption spectra in the visible range is principally consistent with the influence of surface on the measured n. In STO/MgO, the presence of nanometer-sized islands probably results in an additional absorption, clearly seen at $E < 3.5$ eV. Compared to single-crystal STO, surprisingly large absorption in the visible range is observed in STO/$DyScO_3$ (figure 5(b)). In epitaxial STO/$DyScO_3$ films in [7], formation of complicated microstructure with nanosized domains of different types and with various domain boundaries has been demonstrated. Although the reason for the large absorption in STO/$DyScO_3$ is not clear, it might be related to the presence of such domain boundaries.

Similarly to crystal STO, the film of STO/$KTaO_3$ is transparent in the range of $E < 3.5$ eV, which allows one to analyze the near-edge absorption (inset in figure 5(d)). From a good fit to the relationship $[(\alpha)^{1/2} \propto (E - \Delta E)]$, an indication of an indirect gap of about 3.8 eV is found. This is larger than the gaps of 3.29 and 3. 64 eV associated with the indirect R–G and M–G transitions in single-crystal STO. Such a shift of the gap to a higher energy can be explained by the above discussed possible strain-induced FE transition. From comparison of the optical properties of various ultrathin STO films and crystal STO, the following tendencies can be suggested. Compared to single-crystal STO, in the visible range the main contribution to the changes is related to the presence of surfaces including the film's top surface, the film–substrate interface, and some domain boundaries. In the ultraviolet range, the smearing of interband transitions can be related to the small thickness itself. The presence of biaxial strain leads to profound suppression of the interband transitions. The energies of the transitions increase due to the presence of the strain-induced FE state and polarization. In the vicinity of the absorption edge, the film properties are affected by all the mentioned factors (surface, thickness, strain, and polarization) and are difficult to analyze and/or predict.

4. Conclusions

In summary, ultrathin STO films with thickness <15 nm are grown on various single-crystal substrates and their room-temperature crystal structure and optical properties are experimentally analyzed. Epitaxial films with biaxial in-plane strain -0.25 to $+2.1\%$ are obtained on $LaAlO_3$, $DyScO_3$, and $KTaO_3$ substrates. The possibility for abrupt strain relaxation is detected. The critical thickness d_{CRIT} is estimated to be less than 10 nm.

In the spectral range of 1–6 eV, the optical properties of ultrathin STO films with different microstructure and those of single-crystal STO are extracted from the ellipsometric data and compared with each other. In the films, surface effects are suggested to be dominant in the visible range. The interband transitions can be smeared due to small thickness, they can be suppressed due to the presence of biaxial strain, and their energies can increase due to strain-induced polarization. The absorption edge is affected by all the mentioned factors.

Acknowledgments

The work is supported by the Academy of Finland (grant 118250), the Czech Academy of Science (grants AV0Z10100522 and GACR 202/08/1009), and the Russian Academy of Science (grant Sc.Sch.-2628.2008.2 and Program 'Quantum electronics of condensed matter').

References

[1] Menou N *et al* 2008 *Proc. IEEE 2008 Int. Electron Devices Mtg (San Francisco, CA, Dec. 2008)* p 929
[2] Kamalasanan M N, Kumar N D and Chandra S 1993 *J. Appl. Phys.* **74** 679
Kamaras K, Barth K L, Keilmann F, Henn R, Reedyk M, Thomson C, Cardona M, Kircher J, Richards P L and Stehle J L 1995 *J. Appl. Phys.* **78** 1253
Ma J H, Huang Z M, Mang X J, Liu S J, Chang X D, Sun J L, Xue J Q and Chu J H 2006 *J. Appl. Phys.* **99** 033515
Bao D, Yao X, Wakiya N, Shinozaki K and Mizutani N 2001 *Appl. Phys. Lett.* **79** 3767
[3] He F, Wells B O and Shapiro S M 2005 *Phys. Rev. Lett.* **94** 176101
[4] Catalan G, Noheda B, McAneney J, Sinnamon L J and Gregg J M 2005 *Phys. Rev.* B **72** 020102
[5] Pertsev N A, Tagantsev A K and Setter N 2000 *Phys. Rev.* B **61** R825
[6] Haeni J H *et al* 2004 *Nature* **430** 758
[7] Li Y L *et al* 2006 *Phys. Rev.* B **73** 184112
[8] Yamada T *et al* 2006 *Phys. Rev. Lett.* **96** 157602
[9] Vasudevarao A *et al* 2006 *Phys. Rev. Lett.* **97** 257602
[10] Hellwege K H and Hellwege A M (ed) 1981 *LANDOLT-BÖRNSTEIN, Numerical Data and Functional Relationships in Science and Technology* (*New Series, Group III, Crystal and Solid State Physics* vol 16) (Berlin: Springer)
[11] Heifets E, Piskunov S, Kotomin E A, Zhukovskii Y F and Ellis D E 2007 *Phys. Rev.* B **75** 115417 and references therein
[12] Watanabe F, Cahill D G and Greene J E 2005 *Phys. Rev. Lett.* **94** 066101
[13] Dejneka A *et al* 2009 unpublished
[14] Shablayev S I, Danishevsky A M and Subashiev V K 1984 *Sov. Phys. —JETP* **59** 1256